## Title

A continuum damage model based on homogenization of distributed cohesive micro-cracks



**Authors**

Li, Shaofan

Wang, Gang

**Publication Date**

2001-09-01

REPORT
UCB/SEMM-2001/10

STRUCTURAL ENGINEERING
MECHANICS AND MATERIALS

# A Continuum Damage Model Based on Homogenization of Distributed Cohesive Micro-cracks

by

Shaofan Li and Gang Wang



FALL SEMESTER 2001

DEPARTMENT OF CIVIL ENGINEERING
UNIVERSITY OF CALIFORNIA
BERKELEY, CALIFORNIA

# A Continuum Damage Model Based on Homogenization of Distributed Cohesive Micro-cracks

Shaofan Li [1] and Gang Wang [2]

*Department of Civil and Environmental Engineering,*
*University of California, Berkeley, CA 94720 U.S.A.*

**Abstract**

A new continuum damage model is proposed based on homogenization of cohesive micro-cracks in an elastic representative volume element (RVE). A novel damage model is developed to model progressive microrupture and material degradation through cohesive micro-crack coalescence and nucleation. The newly proposed damaged model includes a macro-level yield potential function and the corresponding damaged evolution law, which describes a pressure-sensitive elasto-plastic material at macro-level.

The proposed damage theory is distinctly different from existing damage theories, such as the Gurson's model, which is based on void growth in a perfectly plastic medium. The proposed new damage model is based micromechanics analysis of cohesive crack growth in an elastic medium, which mimics the realistic interactions among atomistic bond forces at micro-level. The underline assumption is that there is a random distribution of Dugdale-Barenblatt cohesive cracks in an elastic RVE. When the RVE is under uniform triaxial tension, the material starts to degrade. The key assumption on homogenization is the equivalence of the maximum distorsional energy. The continuum damage model is then derived through homogenization of a upper bond solution of a cohesive crack embedded in a three dimensional (3D) elastic medium.

**Key Words:** *Cohesive Force, Damage Model, Dugdale-Barenblatt Crack, Elastoplastic Materials, Homogenization, Micromechanics, Micro-crack Distribution, Representative Volume Element, Yield Surface*

[1] Corresponding author, li@ce.berkeley.edu
[2] Graduate Research Assistant, wang@ce.berkeley.edu

## 1 Introduction

Micromechanics modeling, or using homogenization methodologies to derive macro-level constitutive relations that take into account of micro-damage evolution, has been an important subject in reliability analysis to predict material failure and degradation. The well-known Gurson's model (Gurson [16, 17] and Tvergaard [35]) is such an example, in which the material's failure mechanism at micro-level is postulated to be void growth, and the macro-level constitutive relation obtained from homogenization is a pressure sensitive plasticity, which depends on the volume fraction of the void in a representative volume element (RVE). The most distinguished feature of the Gurson's model is that the constitutive relation at micro-level, perfectly plastic in specific, differs from the constitutive relation at macro-level, an associative plasticity with damage-softening. This feature is absent in the early micro-elasticity, where in both micro-level as well as macro-level, constitutive equations are the same, i.e., the linear elasticity — the generalized Hooke's law prevails; homogenization does not produce new constitutive relations at macro-level, which are the primary objectives that are being sought for (see: Eshelby [11, 12], Hashin and Shtrikman [18, 19], and Hill [21], or Mura [29], Nemat-Nasser and Hori [31] for comprehensive review).

In principle, an accurate micromechanics model will lead to an accurate constitutive law at macro-level, provided that a feasible homogenization can be carried out. For the Gurson's model, the void growth mechanism is supported by many experimental observations on failures of ductile materials (see McClintock [28]). On the other hand, in most brittle or quasi-brittle materials such as concrete, rocks, cast irons, and some ceramics, the damage failure mechanism is usually attributed to coalescence and nucleation of micro-cracks. Nonetheless, micro-crack coalescence and nucleation may be attributed to the failure of ductile materials as well (e.g. Rice [33], Rice and Thomson [34] ). Although several micro-crack based damage models have been proposed to describe the brittle failure process (e.g. Krajcinovic [26], Nemat-Nasser and Hori [30]), few micro-crack damage models are available for ductile materials.

Furthermore, the Gurson's model is a phenomenological micro-mechanics model in essence, meaning that in micro-level, the physics law is still phenomenological – the assumption on perfectly plastic medium inside RVE, which is an over-simplified theory.

It is generally believed that on micro-level, or even meso-level, realistic physical constitutive laws should be adopted to model real material behaviors. The cohesive model has been long regarded as a sensible approximation to model fracture, fatigue, and other failure phenomena. Since ultimately, the separation of two solid surfaces is governed by atomistic bond forces, as well as the material's micro-structures at atomistic level.

Since Barenblatt [1, 2] and Dugdale's pioneer contribution [10], the cohesive models have been extensively studied by many authors, e.g. Bilby, Cottrell, and Swinden [7], Becker and Gross [3], Weertman [36], and Feng and Gross [13].

In reality, cohesive zone has a very small length scale, and how to assess the overall effect of cohesive zone degradation is important for study brittle/ductile fracture in macro-level. Recently, the Barenblatt-type model has been implemented in finite element based numerical computations (e.g. Xu et al [37] and Ortiz et al [32]). In their approach, no homogenization procedure has been taken into consideration, and cohesive force only exists between finite element edges. In latest development, some new cohesive models with homogenization features have also been proposed in literature, e.g. Gao and Klein's *Internal Cohesive Bonds* model [14]. Most of these homogenized cohesive models follow a numerical homogenization procedure, i.e. numerical averaging procedure.

In this paper, an analytical homogenization procedure is developed to homogenized an elastic solid with randomly distributed cohesive cracks — Dugdale-Barenlatt crack. The homogenization of cohesive micro-cracks leads to a new damaged evolution law at macro-level. A new pressure sensitive elasto-plastic constitutive relation is obtained, which reflects the accumulated damaged effect due to the distribution of micro-cracks.

## 2 Cohesive Penny-shaped Crack Under Triaxial Tension

Penny-shaped Dugdale crack growth problem has been studied by several authors. The early contribution was made by Keer and Mura [25], who used the Tresca yield criterion to link the maximum axial stress in cohesive zone to the yield stress, or cohesive stress. In their study, only uniaxial tension loading is considered. The problem was studied again by Becker and Gross [5], who studied the cases under both shear and triaxial loadings. In their study, the Von Mises criterion is used in cohesive zone to link the maximum axial stress with the yield stress (cohesive stress). More recently, Chen and Keer [8, 9] revisited the problem, and they obtained the general results for a crack under mixed-mode loading.

On the other hand, however, the problem has not been thoroughly studied from micromechanics perspective. Therefore, the available relationships between maximum tensile stress in process zone as well as yield stress in process zone (cohesive zone) have not been linked to the remote stress on the boundary of a representative volume element — the macro stress.

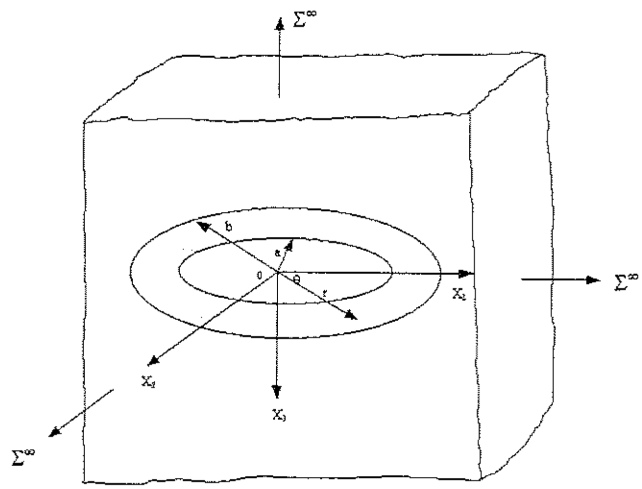


Fig. 1. A penny-shaped cohesive crack in representative volume element (the shaded region: process zone–yielded ring).

By examining a cohesive penny-shaped crack model in a RVE, it may provide complete links among the physical cohesions, yield stress, and remote stresses acting on the boundary of the RVE, which establishes a foundation in homogenization process.

### *2.1 Three-dimensional penny-shaped crack problem*

Consider a three-dimensional penny-shaped Dugdale crack of radius $a$ with a ring-shaped process zone of width b-a in a representative volume element, which may be viewed as an infinite isotropic space by the dwellers in the micro-space.

Let the normal crack surface parallel to $Z$ ($X_3$) axis (see Fig. 1) and a uniform triaxial tension stress is applied at the remote boundary of the RVE, $\Sigma_{ij}^{\infty} = \Sigma^{\infty}\delta_{ij}$. In cylindrical coordinate, the remote traction boundary conditions and displacement boundary condition are expressed as

$$\sigma_{zz}(r,\theta,\infty) = \Sigma^{\infty} \tag{1}$$
$$\sigma_{rr}(\infty,\theta,z) = \Sigma^{\infty} \tag{2}$$
$$\sigma_{\theta\theta}(\infty,\theta,z) = \Sigma^{\infty} \tag{3}$$
$$u_z(r,\theta,0) = 0, \qquad b \le r,\ 0 \le \theta \le 2\pi \tag{4}$$

The stress distribution on the crack surface and process zone

$$\sigma_{zz}(r,\theta,0) = \sigma^0 H(r-a)\ , \quad 0 \le r \le b,\ 0 \le \theta \le 2\pi \tag{5}$$

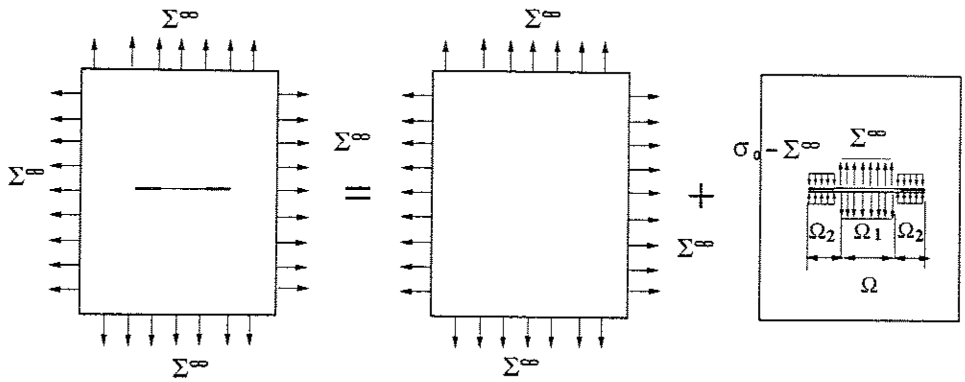


Fig. 2. Illustration of superposition of cohesive crack problem

where $\Sigma^\infty$ is the remote stress, $H(r-a)$ is the Heaviside function, and $\sigma^0$ is the magnitude of cohesion in the process zone, which is different from the yield stress in general. The problem can be viewed as superposition of of two problems: a wholesome RVE with uniform triaxial tension at remote boundary, and a RVE with crack that is subjected the following boundary conditions (see Fig. 2)

$$\sigma_{zz}(r,\theta,\infty)=0 \tag{6}$$
$$\sigma_{rr}(\infty,\theta,z)=0 \tag{7}$$
$$\sigma_{\theta\theta}(\infty,\theta,z)=0 \tag{8}$$
$$\sigma_{zz}(r,\theta,0)=-\Sigma^\infty+\sigma^0 H(r-a)\ , \quad 0<r<b,\ 0\le\theta\le 2\pi \tag{9}$$
$$u_z(r,\theta,0)=0, \qquad b\le r,\ 0\le\theta\le 2\pi \tag{10}$$

Introducing Papkovitch-Neuber displacement potential (see Green and Zener [15] and Kassir and Sih [24]), one may express displacements as follows

$$2\mu u_r=-(1-2\nu)\frac{\partial\Phi}{\partial r}-z\frac{\partial^2\Phi}{\partial r\partial z} \tag{11}$$
$$2\mu u_\theta=-(1-2\nu)\frac{1}{r}\frac{\partial\Phi}{\partial\theta}-\frac{z}{r}\frac{\partial^2\phi}{\partial\theta\partial z} \tag{12}$$
$$2\mu u_z=2(1-\nu)\frac{\partial\Phi}{\partial z}-z\frac{\partial^2\Phi}{\partial z^2} \tag{13}$$

where the potential function is harmonic, i.e. $\nabla^2\Phi=0$. Subsequently strain and stress components may be found as

$$2\mu\epsilon_{rr}=-(1-2\nu)\frac{\partial^2\Phi}{\partial r^2}-z\frac{\partial^3\Phi}{\partial r^2\partial z} \tag{14}$$
$$2\mu\epsilon_{\theta\theta}=-\frac{(1-2\nu)}{r}\frac{\partial\Phi}{\partial r}-\frac{z}{r}\frac{\partial^2\Phi}{\partial r\partial z}-\frac{(1-2\nu)}{r^2}\frac{\partial^2\Phi}{\partial\theta^2}-\frac{z}{r^2}\frac{\partial^2\Phi}{\partial^2\theta\partial z} \tag{15}$$

$$2\mu\epsilon_{zz} = (1-2\nu)\frac{\partial^2\Phi}{\partial z^2} - z\frac{\partial^3\Phi}{\partial z^3} \tag{16}$$

$$2\mu\epsilon_{zr} = -z\frac{\partial^3\Phi}{\partial r\partial z^2} \tag{17}$$

$$2\mu\epsilon_{\theta z} = -\frac{z}{r}\frac{\partial^3\Phi}{\partial\theta\partial z^2} \tag{18}$$

$$2\mu\epsilon_{r\theta} = \frac{1}{r}\Big[\Big(1-2\nu\Big)\Big(\frac{1}{r}\frac{\partial\Phi}{\partial\theta} - \frac{\partial^2\Phi}{\partial\theta\partial r}\Big) + \frac{z}{r}\frac{\partial^2\Phi}{\partial\theta\partial z} - z\frac{\partial^3\Phi}{\partial\theta\partial r\partial z}\Big] \tag{19}$$

and

$$\sigma_{rr} = 2\nu\frac{\partial^2\Phi}{\partial z^2} - (1-2\nu)\frac{\partial^2\Phi}{\partial r^2} - z\frac{\partial^3\Phi}{\partial r^2\partial z} \tag{20}$$

$$\sigma_{\theta\theta} = -\Big[2\nu\frac{\partial^2\Phi}{\partial r^2} + \frac{1}{r}\frac{\partial\Phi}{\partial r} + \frac{1}{r^2}\frac{\partial^2\Phi}{\partial\theta^2} + \frac{z}{r}\frac{\partial^2\Phi}{\partial r\partial z} + \frac{z}{r^2}\frac{\partial^3\Phi}{\partial\theta^2\partial z}\Big] \tag{21}$$

$$\sigma_{zz} = \frac{\partial^2\Phi}{\partial z^2} - z\frac{\partial^3\Phi}{\partial z^3} \tag{22}$$

$$\sigma_{zr} = -z\frac{\partial^3\Phi}{\partial r\partial z^2} \tag{23}$$

$$\sigma_{z\theta} = -\frac{z}{r}\frac{\partial^3\Phi}{\partial\theta\partial z^2} \tag{24}$$

$$\sigma_{r\theta} = \frac{1}{r}\Big[(1-2\nu)\Big(\frac{1}{r}\frac{\partial\Phi}{\partial\theta} - \frac{\partial^2\Phi}{\partial\theta\partial r}\Big) + z\Big(\frac{1}{r}\frac{\partial^2\Phi}{\partial\theta\partial z} - \frac{\partial^3\Phi}{\partial\theta\partial r\partial z}\Big)\Big] \tag{25}$$

By Hankel transform and only consider the symmetric mode, one may have

$$\begin{cases} \bar{\Phi}(\xi,z) = \int_0^\infty r\Phi(r,z)J_0(\xi r)dr \\ \\ \Phi(r,z) = \int_0^\infty \xi\bar{\Phi}(\xi,z)J_0(\xi r)d\xi \end{cases} \tag{26}$$

and

$$\nabla^2\Phi = 0 \quad \Rightarrow \quad \Big(\frac{d^2}{dz^2} - \xi^2\Big)\bar{\Phi}(\xi,z) = 0\ . \tag{27}$$

Eq. (27) yields solution

$$\bar{\Phi}(\xi,z) = \bar{A}(\xi)\exp(-\xi z) + \bar{B}(\xi)\exp(\xi z)\ , \qquad (\xi > 0) \tag{28}$$

Consider the remote boundary conditions and let

$$\bar{B}(\xi) = 0 \tag{29}$$
$$\bar{A}(\xi) = -\xi^{-2} A(\xi) \ . \tag{30}$$

The displacement potential may be expressed as

$$\Phi(r,z) = -\int_0^\infty \xi^{-1} A(\xi) \exp(-\xi z) J_0(\xi r) d\xi \ . \tag{31}$$

Then the boundary conditions (9) and (10) render the following dual integral equations

$$\begin{cases} \displaystyle\int_0^\infty \xi A(\xi) J_0(\xi r) d\xi = \Sigma^\infty - \sigma^0 H(r-a), & 0 < r < b \\ \\ \displaystyle\int_0^\infty A(\xi) J_0(\xi r) d\xi = 0, & r \geq b \end{cases} \tag{32}$$

Let

$$A(\xi) = \int_0^b \phi(t) \sin \xi t dt \tag{33}$$

where $\phi(t)$ is yet to be determined. The arrangement will automatically satisfy displacement boundary condition,

$$2\mu u_z(r,\theta,0) = 2(1-\nu) \int_0^\infty A(\xi) J_0(\xi r) d\xi = 0, \ \ \forall \ r > b \tag{34}$$

Solving (32), one may obtain

$$\phi(t) = \begin{cases} \dfrac{2}{\pi} \Sigma^\infty t & t < a \\ \\ \dfrac{2}{\pi} \left( \Sigma^\infty t - \sigma^0 \sqrt{t^2 - a^2} \right) & a < t < b \end{cases} \tag{35}$$

The size of the process zone, $a/b$, remote stress $\Sigma^\infty$, and cohesion, $\sigma^0$ are related through expression to ensure stresses at the crack tip to be finite,

$$\frac{a}{b} = \sqrt{1 - \frac{(\Sigma^\infty)^2}{(\sigma^0)^2}} \qquad \text{or} \qquad \frac{\Sigma^\infty}{\sigma^0} = \sqrt{1 - \frac{a^2}{b^2}} \tag{36}$$

There are several ways to determine the critical cohesion in the process zone: (1) Let $\sigma^0 = \sigma_Y$, where $\sigma_Y$ is the yield stress of virgin material under uniaxial tension; (2) Use Tresca criterion in the process zone [25, 29]; and (3) Use Von Mises criterion in the process zone [6].

In this paper, the third approach is adopted to link the physical cohesion $\sigma^0$ with the true yield stress of a virgin material, $\sigma_Y$.

After some calculation, one may find that in the yield ring (process zone), $z = 0$ and $a < r < b$,

$$\sigma_{zz} = \sigma^0 - \Sigma^\infty \tag{37}$$

$$\begin{aligned}\sigma_{rr} &= -(1-2\nu)\frac{\partial^2 \Phi}{\partial r^2} + 2\nu\frac{\partial^2 \Phi}{\partial z^2} \\ &= -\frac{1+2\nu}{2}\Sigma^\infty + \Big[\frac{1-2\nu}{2}\Big(1+\frac{a^2}{r^2}\Big) + 2\nu\Big]\sigma^0\end{aligned} \tag{38}$$

$$\begin{aligned}\sigma_{\theta\theta} &= -\Big(\frac{1}{r}\frac{\partial \Phi}{\partial r} + 2\nu\frac{\partial^2 \Phi}{\partial r^2}\Big) \\ &= -\frac{1+2\nu}{2}\Sigma^\infty + \Big[\frac{1-2\nu}{2}(1-\frac{a^2}{r^2}) + 2\nu\Big]\sigma^0\end{aligned} \tag{39}$$

Assume that $\dfrac{a^2}{b^2} \approx 1$ and $a \leq r \leq b$. Thus $\dfrac{a^2}{r^2} \approx 1$. Within the process zone, the total stresses are

$$\sigma_{zz} = \sigma^0 \tag{40}$$

$$\sigma_{rr} = \frac{1-2\nu}{2}\Sigma^\infty + \sigma^0 \tag{41}$$

$$\sigma_{\theta\theta} = \frac{1-2\nu}{2}\Sigma^\infty + 2\nu\sigma^0 \tag{42}$$

Following Lu and Chow [27] to link the physical cohesion to the true yield stress $\sigma_Y$ inside the process zone, we substitute Eqs. 40–42 into the von-Mises criterion,

$$\frac{1}{2}\Big[(\sigma_{rr} - \sigma_{zz})^2 + (\sigma_{\theta\theta} - \sigma_{zz})^2 + (\sigma_{rr} - \sigma_{\theta\theta})^2\Big] = \sigma_Y^2 \tag{43}$$

It leads the following quadratic equation,

$$4\Big(\frac{\sigma^0}{\Sigma^\infty}\Big)^2 - 2\Big(\frac{\sigma^0}{\Sigma^\infty}\Big) + 1 - \Big(\frac{2}{1-2\nu}\frac{\sigma_Y}{\Sigma^\infty}\Big)^2 = 0 \tag{44}$$

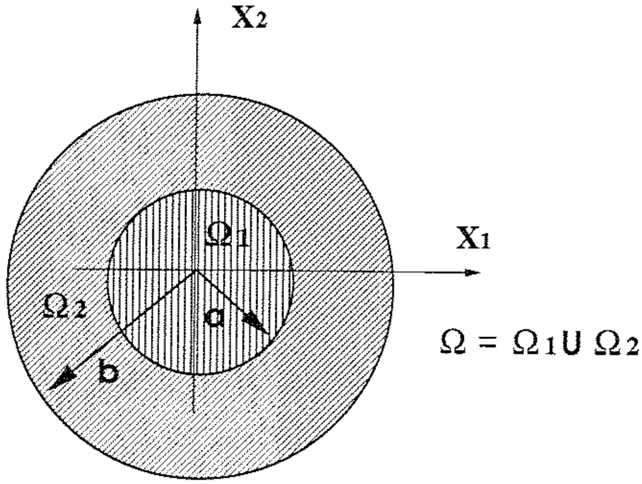


Fig. 3. Projection domain of crack surface and process zone.

Solving the quadratic equation for $\frac{\sigma^0}{\Sigma^\infty}$ yields two roots. The positive root is

$$\frac{\sigma^0}{\Sigma^\infty} = \frac{1+\sqrt{\left(\frac{4}{1-2\nu}\frac{\sigma_Y}{\Sigma^\infty}\right)^2 - 3}}{4} \tag{45}$$

*2.2 Crack opening displacement*

Consider

$$2\mu u_z(r,\theta,0) = 2(1-\nu)\frac{\partial \Phi}{\partial z} = \frac{1-\nu}{\mu}\int_r^b \frac{\phi(t)}{\sqrt{t^2-r^2}}dt$$

$$= \begin{cases} \frac{2}{\pi}\left(\frac{1-\nu}{\mu}\right)\left(\Sigma^\infty\sqrt{b^2-r^2} - \sigma^0\int_a^b \frac{\sqrt{t^2-a^2}}{\sqrt{t^2-r^2}}dt\right) & 0<r<a \\ \\ \frac{2}{\pi}\left(\frac{1-\nu}{\mu}\right)\left(\Sigma^\infty\sqrt{b^2-r^2} - \sigma^0\int_r^b \frac{\sqrt{t^2-a^2}}{\sqrt{t^2-r^2}}dt\right) & a<r<b \end{cases} \tag{46}$$

Define

$$[u_z] = u_z^+ - u_z^- = 2u_z \tag{47}$$

The integration is over the projected area of elastic crack surface on $X_1OX_2$ plane, $\Omega_1$, $(0 \le r \le a)$ is

$$
\begin{aligned}
\int_{\Omega_1}[u_z]dA &= \frac{8(1-\nu)}{\mu}\Big(\Sigma^\infty\int_0^a\sqrt{b^2-r^2}rdr-\sigma^0\int_0^b\int_a^b\frac{\sqrt{t^2-a^2}}{\sqrt{t^2-r^2}}rdtdr\Big)\\
&= \frac{8(1-\nu)}{3\mu}\Big\{\Sigma^\infty\Big[b^3-(b^2-a^2)^{\frac{3}{2}}\Big]-\sigma^0\Big[\Big(b^2-a^2\Big)^{\frac{3}{2}}-(b^3-3a^2b+2a^3)\Big]\Big\}
\end{aligned}
\tag{48}
$$

The integration is over the yielding ring $\Omega_2$, $(a < r < b)$, i.e.

$$
\begin{aligned}
\int_{\Omega_2}[u_z]dA &= \frac{8(1-\nu)}{\mu}\Big[\Sigma^\infty\int_a^b\sqrt{b^2-r^2}rdr-\sigma^0\int_a^b\int_r^b\frac{\sqrt{t^2-a^2}}{\sqrt{t^2-r^2}}rdtdr\Big]\\
&= \frac{8(1-\nu)}{3\mu}\Big[\Sigma^\infty(b^2-a^2)^{\frac{3}{2}}-\sigma^0(b^3-3a^2b+2a^3)\Big]
\end{aligned}
\tag{49}
$$

The volume of a single crack opening is integrated over the projection of the entire crack surface on $X_1OX_2$ plane, $\Omega = \Omega_1 \cup \Omega_2$,

$$
\begin{aligned}
V_c &= \int_{\Omega}[u_z]dA = \int_{\Omega_1}[u_z]dA + \int_{\Omega_2}[u_z]dA\\
&= \frac{8(1-\nu)}{3\mu}b^3\Big[\Sigma^\infty-\sigma^0\Big(1-(\frac{a}{b})^2\Big)^{\frac{3}{2}}\Big]\\
&= \frac{8(1-\nu)}{3\mu}a^3\Big(\frac{b}{a}\Big)^3\Big[\Sigma^\infty-\sigma^0\Big(\frac{\Sigma^\infty}{\sigma^0}\Big)^3\Big]\\
&= \frac{8(1-\nu)}{3\mu}a^3\frac{\Sigma^\infty}{\sqrt{1-\Big(\frac{\Sigma^\infty}{\sigma^0}\Big)^2}}
\end{aligned}
\tag{50}
$$

## 3 Average Theorem

Since the cohesive crack is not a traction-free defect, the available averaging theorem for traction-free defects may not be applicable to homogenizations of cohesive defects.

In this section, an averaging theorem is proved for elastic solids having process zones with constant cohesion.

Before proceed to prove a general averaging theorem, we consider the average stress in an three-dimensional (3D) elastic representative volume element with a single penny-shaped Dugdale-Barrenblatt crack at the center of the RVE.

Denote the elastic crack surface as $\partial V_{ec} = \partial V_{ec+} \cup \partial V_{ec-}$ and its projection onto $X_1X_2$ plane as $\Omega_1$. Denote the cohesive process zone (ring shape) as $\partial V_{pz} = \partial V_{pz+} \cup \partial V_{pz-}$ and its projection onto $X_1X_2$ plane as $\Omega_2$. In addition, $V_c = V_{ec} \cup V_{pz}$ and $\Omega = \Omega_1 \cup \Omega_2$ Assume that there is no body force present. Using divergence theorem, it is straightforward that

$$
\begin{aligned}
< \sigma_{ij} > &= \frac{1}{V}\int\limits_V \sigma_{ij} dV = \frac{1}{V}\int\limits_V \left(\sigma_{kj}x_i\right)_{,k} dV \\
&= \frac{1}{V}\left\{\int\limits_V \Sigma^\infty_{kj} x_i n_k dS - \int\limits_{\partial V_{ec}} 0 \cdot x_i n_k dS - \int\limits_{\partial V_{pz}} \sigma_{kj} x_i n_k dS\right\} \\
&= \Sigma^\infty_{ij} - \frac{1}{V}\int\limits_{\partial V_{pz}} \sigma_{kj} x_i n_k dS = \Sigma^\infty_{ij} - \frac{1}{V} t^0_j \int\limits_{\partial V_{pz}} x_i dS
\end{aligned} \tag{51}
$$

where $t^0_j$ is the constant cohesive traction. If the cohesion does not have shear component, then $\{t^0_j\} = (0, 0, \sigma^0)$ where $\sigma^0$ is the magnitude of physical cohesion in the process zone.

Since the cohesive ring lies on $X_1X_2$ plane,

$$
\int\limits_{\partial V_{pz}} x_3 dS = 0, \tag{52}
$$

By symmetry, inside the cohesive ring

$$
\int\limits_{\partial V_{pz}} x_i dS = 0, \quad i = 1, 2 \tag{53}
$$

Therefore, the average stress inside the RVE will equal to remote stress

$$
< \sigma_{ij} > = \Sigma^\infty_{ij} - \frac{1}{V} t^0_j \int\limits_{\partial V_{pz}} x_i dS = \Sigma^\infty_{ij} \tag{54}
$$

Now consider an 3D RVE with N random distributed cohesive cracks with the same size. Each of them is associated with a same size cohesive ring. Suppose that they are all aligned in $X_3$ direction. The average stress inside the RVE then would be

$$
< \sigma_{ij} > = \frac{1}{V}\int\limits_V \sigma_{ij} dV = \frac{1}{V}\int\limits_V \left(\sigma_{kj}x_i\right)_{,k} dV
$$

$$= \frac{1}{V}\left\{ \int_V \Sigma_{kj}^{\infty} x_i n_k dS - \sum_{\alpha=1}^{N} \int_{\partial V_{ec\alpha}} 0 \cdot x_i n_k dS - \sum_{\alpha=1}^{N} \int_{\partial V_{pz\alpha}} \sigma_{kj} x_i n_k dS \right\}$$

$$= \Sigma_{ij}^{\infty} - \frac{1}{V} \sum_{\alpha=1}^{N} \int_{\partial V_{pz\alpha}} \sigma_{kj} x_i n_k dS \tag{55}$$

$$= \Sigma_{ij}^{\infty} - \frac{1}{V} \sum_{\alpha=1}^{N} t_j^{(\alpha)0} \int_{\partial V_{pz\alpha}} x_i dS \tag{56}$$

Assume that the center of a cohesive ring is located at $(x_{\alpha 1}, x_{\alpha 2}, x_{\alpha 3})$. Introduce local coordinate $x_i'$ such that $x_i = x_{\alpha i} + x_i'$. Eq. (56) becomes

$$< \sigma_{ij} >= \Sigma_{ij} - \frac{1}{V} \sum_{\alpha=1}^{N} t_j^{(\alpha)0} \Big( x_{\alpha i} |\partial V_{pz\alpha}| + \int_{\partial V_{pz\alpha}} x_i' dS \Big) \tag{57}$$

In each local coordinate system, $\int_{\partial V_{pz\alpha}} x_i' dS = 0$, because of the symmetry. Assume that the crack distribution is uniform (axisymmetric) in the RVE. A reasonable assumption would be

$$\sum_{\alpha} x_{\alpha i} = 0, \quad i = 1, 2, 3 \tag{58}$$

In fact, one can assume that there is an axisymmetric crack distribution function $w(\mathbf{x}) = w_z(z) w_r(r) w_\theta(\theta)$ with $w_\theta(\theta) = 1$ such that

$$\int_V w(\mathbf{x}) dV = 2\pi \int_{-\infty}^{\infty} w_z(z) dz \int_0^{\infty} w_r(r) r dr = N \tag{59}$$

where $N$ is the total number of cracks and $w_\theta(\theta) = 1$. It is then statistically equivalent

$$\sum_{\alpha} x_{\alpha j} = \int_V x_{\alpha j} w(\mathbf{x}) dV \tag{60}$$

It is trivial to show that the last integral is actually zero, because $w_z(z)$ must be an even function, and $w_z(z) z$ has to be an odd function. Therefore,

$$\int_{-\infty}^{+\infty} w_z(z) z dz = 0 \quad \Rightarrow \quad \int_V x_{\alpha j} w(\mathbf{x}) dV = 0, \tag{61}$$

provided $w_z(z)z$ is integrable. In addition, it is also obvious that

$$\int_0^{2\pi} \left\{ \begin{array}{c} x_{\alpha 1} \\ x_{\alpha 2} \end{array} \right\} d\theta = \int_0^{2\pi} r \left\{ \begin{array}{c} \cos\theta \\ \sin\theta \end{array} \right\} d\theta = 0 \tag{62}$$

Considering $|\partial V_{pz\alpha}| = |\partial V_{pz}| = const.$, for $\alpha = 1, 2, \cdots, N$, one may conclude that

$$< \sigma_{ij} >= \Sigma_{ij}^{\infty} \tag{63}$$

In general, cracks in a RVE may not to be aligned with $Z$ or $X_3$ direction. In this case, we have the following statement.

**Theorem 3.1** *Suppose that an elastic representative volume element contains $N$ traction-free cracks and $N$ cohesive damaged process zones with constant cohesive traction. Suppose that the cohesive crack distribution is isotropic and there is no shear cohesive force on the surface on the process zone. If the traction on the remote boundary of the RVE is generated by a constant stress tensor, $\Sigma_{ij}^{\infty}$, i.e, $t_i^{\infty} = n_j \Sigma_{ji}^{\infty}$, the average stress inside the RVE satisfies*

$$< \sigma_{ij} >= \Sigma_{ij}^{\infty} \tag{64}$$

**Proof:**

As shown above

$$< \sigma_{ij} >= \Sigma_{ij}^{\infty} - \frac{1}{V} \sum_{\alpha=1}^{N} \int_{\partial V_{pz\alpha}} t_j^{(\alpha)0} x_i dS \tag{65}$$

Let $x_i = x_{\alpha i} + x'_{\alpha i}$, where $x_{\alpha i}$ is the coordinate for the center of process zone $\alpha$. By symmetry,

$$\int_{\partial V_{pz\alpha}} x'_{\alpha j} dS = 0 \tag{66}$$

This is valid in any crack orientation. Therefore

$$< \sigma_{ij} >= \Sigma_{ij}^{\infty} - \frac{1}{V} \sum_{\alpha=1}^{N} t_j^{(\alpha)0} x_{\alpha i} |\partial V_{pz\alpha}| \tag{67}$$

Suppose that the distribution, or probability of the crack orientation is random, or isotropic for a given crack $\alpha$ (see Fig. 4). Eq. (67) may be rewritten

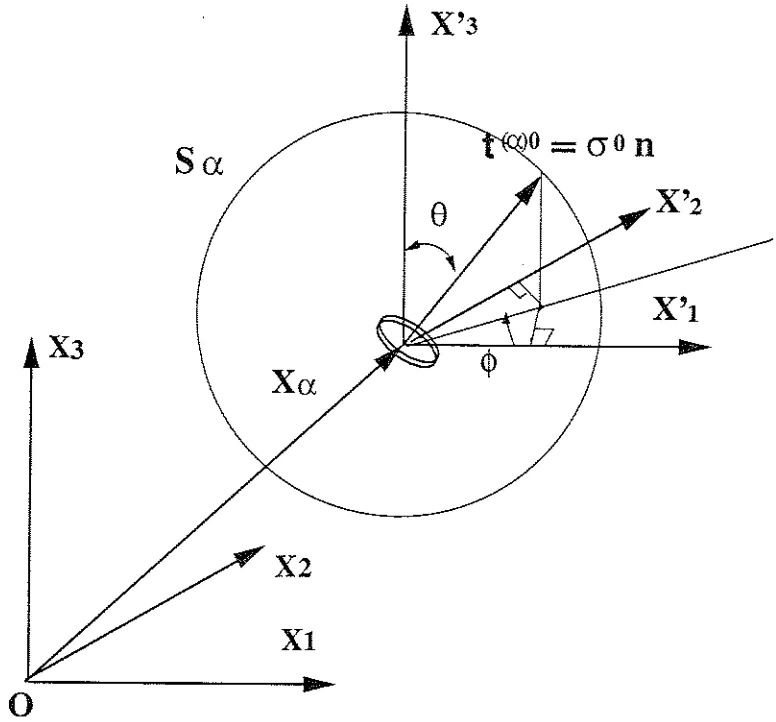


Fig. 4. Isotropic distribution of cracks with different orientations

as

$$< \sigma_{ij} > = \Sigma_{ij}^{\infty} - \frac{1}{V}\sum_{\alpha=1}^{N}\frac{|\partial V_{pz\alpha}|}{4\pi}\int_{S_\alpha} t_j^{(\alpha)0} x_{\alpha i} dS$$

$$= \Sigma_{ij}^{\infty} - \frac{1}{V}\sum_{\alpha=1}^{N}\frac{x_{\alpha i}}{4\pi}|\partial V_{pz\alpha}|\int_0^{\pi}\int_0^{2\pi} t_j^{(\alpha)0}\sin\theta d\theta d\phi \qquad (68)$$

Here $S_\alpha$ is a unit sphere surrounding the cohesive ring, $\alpha$, at center $x_{\alpha i}$.

Let the out normal of crack surface point at $\mathbf{x}_\alpha$ be $\mathbf{n}$. And $\mathbf{t} = \sigma^0\mathbf{n}$, where $\sigma^0$ is the physical cohesion. By assumption that there is no shear cohesive force, one may write the components of $\mathbf{t}^{(\alpha)0}$ as

$$t_1^{(\alpha)0} = \sigma^0 \sin\theta\cos\phi \qquad (69)$$

$$t_2^{(\alpha)0} = \sigma^0 \sin\theta\sin\phi \qquad (70)$$

$$t_3^{(\alpha)0} = \sigma^0 \cos\theta \qquad (71)$$

It is trivial to show

$$\frac{1}{4\pi}\int_0^{\pi}\int_0^{2\pi} t_j^{(\alpha)0}\sin\theta d\theta d\phi = 0, \qquad j = 1, 2, 3 \qquad (72)$$

Thereby,

$$< \sigma_{ij} >= \Sigma_{ij}^{\infty} \tag{73}$$

On the other hand, for a fixed crack orientation, i.e. $\mathbf{t}^{(\alpha)0} = \mathbf{t}^{(\beta)0}$ for $\alpha \neq \beta$. One may show that there exists a spatial distribution function, such that

$$\int_V \sum_{\alpha=1}^{N} x_{\alpha i} w(\mathbf{x}) dV = 0 \tag{74}$$

which is the case of aligned crack distribution proved above. ♣

## 4 Additional Strain Formula

For an elastic solid containing cohesive cracks, it can no longer be viewed as a medium containing traction-free defects, because constant tractions are present on the surfaces of process zones. Hence the conventional elastic additional formula (Vakulenko-Kachanov formula),

$$\boldsymbol{\epsilon}^c = \frac{1}{2V} \int_\Omega \Big( \mathbf{n} \otimes [\mathbf{u}] + [\mathbf{u}] \otimes \mathbf{n} \Big) dV \tag{75}$$

can not be applied in this situation.

In fact, Becker and Gross [4] have studied the additional strain formula for solids containing cohesive cracks by analyzing energy release density for a solid containing cohesive cracks. However, after all the analysis, they derived the same additional strain formula just as in the case of traction-free defect.

In this paper, present authors revisited the problem by using the same energy release density approach. An entirely different additional strain formula is obtained.

To derive the additional strain formula for an elastic solid containing defects with constant traction, we assume that there exit average potential energy density and average complementary potential energy density, which are potential functions of average strain and average stress. Consider the potential energy density for a RVE with a single cohesive crack. Following Becker and Gross [4], the average potential energy density may be viewed as inner product the average stress and average strain subtracting the average complementary potential energy density of undamaged RVE in a uniform stress state and the average energy release density (see Fig. 2)

$$
\begin{aligned}
\tilde{W} &= <\sigma_{ij}><\epsilon_{ij}> - \frac{1}{2}D_{ijk\ell}\Sigma_{ij}^{\infty}\Sigma_{k\ell}^{\infty} - \frac{1}{V}\int\limits_{\partial V_c}\Sigma_{ij}^{\infty}n_i u_j dS + \frac{1}{V}\int\limits_{\partial V_{pz}}\sigma_{ij}^{0}n_i u_j dS \\
&= <\sigma_{ij}><\epsilon_{ij}> - \frac{1}{2}D_{ijk\ell}\Sigma_{ij}^{\infty}\Sigma_{k\ell}^{\infty} - \frac{1}{V}\int\limits_{\partial V_{c+}}\Sigma^{\infty}[u_z]dS + \frac{1}{V}\int\limits_{\partial V_{pz+}}\sigma^{0}[u_z]dS
\end{aligned} \tag{76}
$$

where $\Sigma_{ij}^{\infty} = \Sigma^{\infty}\delta_{ij}$, and the bracket $< \cdot >$ is the standard average operator defined as

$$
<\mathcal{A}> := \frac{1}{V}\int\limits_{V}\mathcal{A}dV \tag{77}
$$

By Legendre transform, the average complementary potential energy will be

$$
\tilde{W}^c := <\sigma_{ij}><\epsilon_{ij}> - \tilde{W} \tag{78}
$$

Therefore,

$$
\tilde{W}^c = \frac{1}{2}D_{ijk\ell}\Sigma_{ij}^{\infty}\Sigma_{k\ell}^{\infty} + \frac{1}{V}\int\limits_{\partial V_{c+}}\Sigma^{\infty}[u_z]dS - \frac{1}{V}\int\limits_{\partial V_{pz+}}\sigma^{0}[u_z]dS \tag{79}
$$

By the hypothesis that $\tilde{W}^c$ is a potential function of $<\sigma_{ij}>$ and by the averaging Theorem 3.1, $\Sigma_{ij}^{\infty} = <\sigma_{ij}>$, one may find

$$
\begin{aligned}
<\epsilon_{ij}> &= \frac{\partial \tilde{W}^c}{\partial <\sigma_{ij}>} = \frac{\partial \tilde{W}^c}{\partial \Sigma_{ij}^{\infty}} \\
&= D_{ijk\ell}\Sigma_{k\ell}^{\infty} + \frac{\partial}{\Sigma_{ij}^{\infty}}\Big(\frac{1}{V}\int\limits_{\partial V_{c+}}\Sigma^{\infty}[u_z]dS - \frac{1}{V}\int\limits_{\partial V_{pz+}}\sigma^{0}[u_z]dS\Big) \\
&= \epsilon_{ij}^{0} + \epsilon_{ij}^{c}
\end{aligned} \tag{80}
$$

where $\epsilon_{ij}^{0} := D_{ijk\ell} < \sigma_{k\ell} >$ and

$$
\begin{aligned}
\epsilon_{ij}^{c} &= \frac{\partial}{\partial \Sigma_{ij}^{\infty}}\Big(\frac{1}{V}\int\limits_{\Omega}\Sigma^{\infty}[u_z]dS - \frac{1}{V}\int\limits_{\Omega_2}\sigma^{0}[u_z]dS\Big) \\
&= \frac{\partial}{\partial \Sigma^{\infty}}\Big(\frac{1}{V}\int\limits_{\Omega}\Sigma^{\infty}[u_z]dS - \frac{1}{V}\int\limits_{\Omega_2}\sigma^{0}[u_z]dS\Big)\frac{\partial \Sigma^{\infty}}{\partial \Sigma_{ij}^{\infty}} \\
&= \frac{\partial}{\partial \Sigma^{\infty}}\Big(\frac{1}{V}\int\limits_{\Omega}\Sigma^{\infty}[u_z]dS - \frac{1}{V}\int\limits_{\Omega_2}\sigma^{0}[u_z]dS\Big)\delta_{ij}
\end{aligned} \tag{81}
$$

Considering an upper bound approximation by neglecting the dissipation term

$$\frac{1}{V}\frac{\partial}{\partial\Sigma^\infty}\left\{\int\limits_{\Omega_2}\sigma^0[u_z]dS\right\}\delta_{ij} \tag{82}$$

and utilizing the result obtained in Eq. (50), one may derive that

$$\epsilon^c_{ij}=\frac{\partial}{\partial\Sigma^\infty}\left\{\frac{8(1-\nu)}{3\nu}\frac{(\Sigma^\infty)^2a^3}{\sqrt{1-(\frac{\Sigma^\infty}{\sigma^0})^2}}\right\}\delta_{ij} \tag{83}$$

Finally, the additional strain formula for a RVE with cohesive defects under uniform triaxial tension is obtained,

$$\epsilon^c_{ij}=\frac{8(1-\nu)}{3\mu}\frac{a^3}{V}\frac{2-\left(\frac{\Sigma^\infty}{\sigma^0}\right)^2}{\left(1-\left(\frac{\Sigma^\infty}{\sigma^0}\right)^2\right)^{3/2}}\Sigma^\infty\delta_{ij} \tag{84}$$

If there are $N$ randomly distributed cracks in an RVE, the additional strain will be

$$\epsilon^c_{ij}=\frac{8(1-\nu)}{3\mu}\sum_{\alpha=1}^{N}\frac{a^3_\alpha}{V}\frac{2-\left(\frac{\Sigma^\infty}{\sigma^0}\right)^2}{\left(1-\left(\frac{\Sigma^\infty}{\sigma^0}\right)^2\right)^{3/2}}\Sigma^\infty\delta_{ij} \tag{85}$$

Define crack opening space volume fraction

$$f:=\sum_{\alpha=1}^{N}\frac{a^3_\alpha}{V} \tag{86}$$

Note that $a^3_\alpha$ is not the exact crack opening volume of the $\alpha$-th crack, and it may be only proportional to the crack opening volume of the $\alpha$-th crack, but it serves well as an index for the measurement of crack opening volume, or being a pseudo crack opening volume.

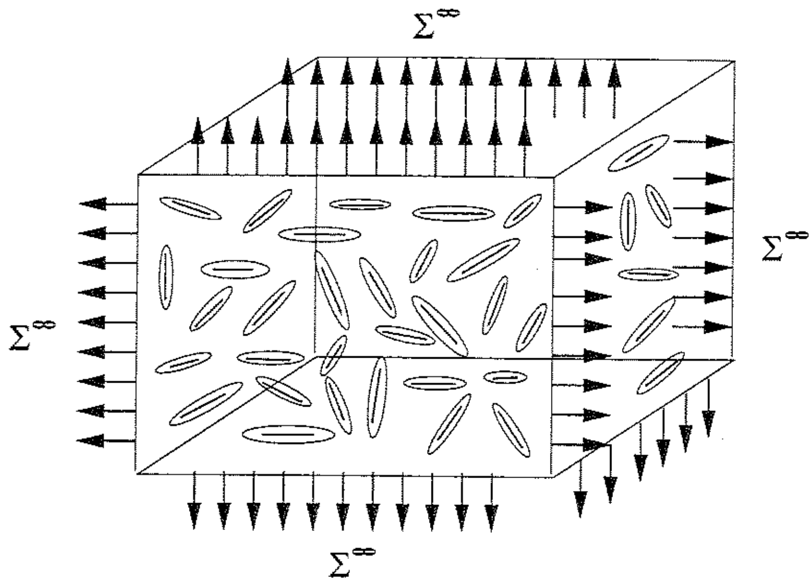


Fig. 5. An RVE with randomly distributed micro-cracks

## 5 Micro-crack damage model

Using Voigt notation and following Nemat-Nasser and Hori [1999], one may derive an expression for **H** tensor

$$\boldsymbol{\epsilon}^c = \mathbf{H} : \boldsymbol{\Sigma} \quad \Rightarrow \begin{bmatrix} \epsilon^c_{11} \\ \epsilon^c_{22} \\ \epsilon^c_{33} \\ 0 \\ 0 \\ 0 \end{bmatrix} = \frac{8(1-\nu)}{3\mu} f \frac{2 - \left(\frac{\Sigma^\infty}{\sigma^0}\right)^2}{\left[1 - \left(\frac{\Sigma^\infty}{\sigma^0}\right)^2\right]^{3/2}} \begin{bmatrix} 1&0&0&0&0&0 \\ 0&1&0&0&0&0 \\ 0&0&1&0&0&0 \\ 0&0&0&h&0&0 \\ 0&0&0&0&h&0 \\ 0&0&0&0&0&h \end{bmatrix} \begin{bmatrix} \Sigma^\infty_{11} \\ \Sigma^\infty_{22} \\ \Sigma^\infty_{33} \\ 0 \\ 0 \\ 0 \end{bmatrix} \tag{87}$$

where parameter $h$ is yet to be determined. From (87), **H** tensor is deduced in a matrix form

$$[\mathbf{H}] = \frac{8(1-\nu)}{3\mu} f \frac{2 - \left(\frac{\Sigma^\infty}{\sigma^0}\right)^2}{\left[1 - \left(\frac{\Sigma^\infty}{\sigma^0}\right)^2\right]^{3/2}} \begin{bmatrix} 1&0&0&0&0&0 \\ 0&1&0&0&0&0 \\ 0&0&1&0&0&0 \\ 0&0&0&h&0&0 \\ 0&0&0&0&h&0 \\ 0&0&0&0&0&h \end{bmatrix} \tag{88}$$

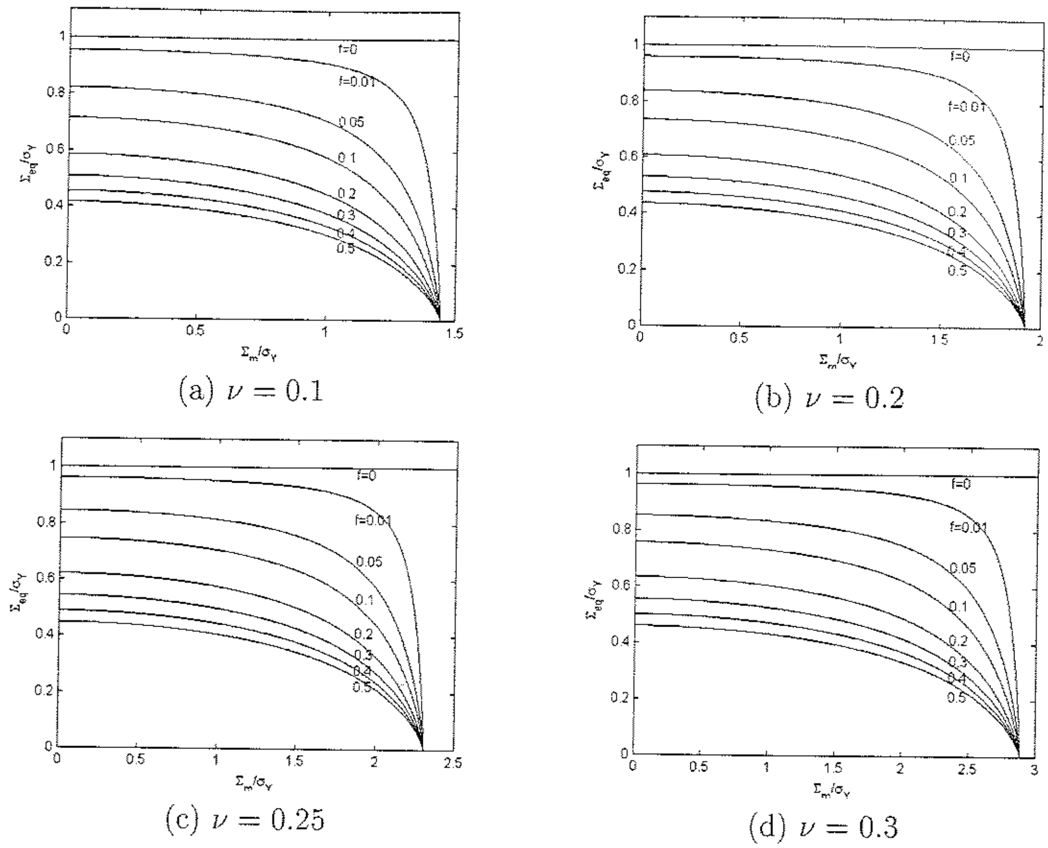


(a) $\nu = 0.1$ (b) $\nu = 0.2$

(c) $\nu = 0.25$ (d) $\nu = 0.3$

Fig. 6. Damaged yield surfaces with different Poisson's ratio

**Remark 5.1** **1.** *Since the far-field is isotropic and hydrostatic, there is no shear deformation inside the RVE.*

**2.** *Since cohesive cracks are uniformly distributed inside RVE, the damaged continuum remains isotropic. There is no need for rotational operation, i.e. Kachanov [1992,1994] [22, 23], Nemat-Nasser and Hori [1999] [31], to homogenize the* **H** *tensor.*

Since **H** tensor is isotropic, the damaged compliance tensor can then be obtained in straightforward fashion,

$$\bar{\mathbf{D}} = \mathbf{D} + \mathbf{H} \tag{89}$$

The Vogit representation of compliance tensor is

$$[\bar{\mathbf{D}}] = \begin{bmatrix} \frac{1}{\bar{E}} & -\frac{\bar{\nu}}{\bar{E}} & -\frac{\bar{\nu}}{\bar{E}} & 0 & 0 & 0 \\ -\frac{\bar{\nu}}{\bar{E}} & \frac{1}{\bar{E}} & -\frac{\bar{\nu}}{\bar{E}} & 0 & 0 & 0 \\ -\frac{\bar{\nu}}{\bar{E}} & -\frac{\bar{\nu}}{\bar{E}} & \frac{1}{\bar{E}} & 0 & 0 & 0 \\ 0 & 0 & 0 & \bar{\mu} & 0 & 0 \\ 0 & 0 & 0 & 0 & \bar{\mu} & 0 \\ 0 & 0 & 0 & 0 & 0 & \bar{\mu} \end{bmatrix} \tag{90}$$

and

$$[\mathbf{D}] = \begin{bmatrix} \frac{1}{E} & -\frac{\nu}{E} & -\frac{\nu}{E} & 0 & 0 & 0 \\ -\frac{\nu}{E} & \frac{1}{E} & -\frac{\nu}{E} & 0 & 0 & 0 \\ -\frac{\nu}{E} & -\frac{\nu}{E} & \frac{1}{E} & 0 & 0 & 0 \\ 0 & 0 & 0 & \mu & 0 & 0 \\ 0 & 0 & 0 & 0 & \mu & 0 \\ 0 & 0 & 0 & 0 & 0 & \mu \end{bmatrix} \tag{91}$$

Since the continuum is isotropic before damage, during damage, and after damage, it is reasonable to assume that

$$\bar{\mu} = \frac{\bar{E}}{2(1+\bar{\nu})} \tag{92}$$

From (92), one can determine $h$ from $h = \bar{\mu} - \mu$.

Solving Eq. (89) yields

$$\frac{1}{\bar{E}} = \frac{1}{E} + \frac{4(1-\nu)}{3\mu} f \frac{2 - \left(\frac{\Sigma^\infty}{\sigma^0}\right)^2}{\left[1 - \left(\frac{\Sigma^\infty}{\sigma^0}\right)^2\right]^{3/2}} \tag{93}$$

$$\frac{\bar{\nu}}{\bar{E}} = \frac{\nu}{E} \tag{94}$$

Therefore,

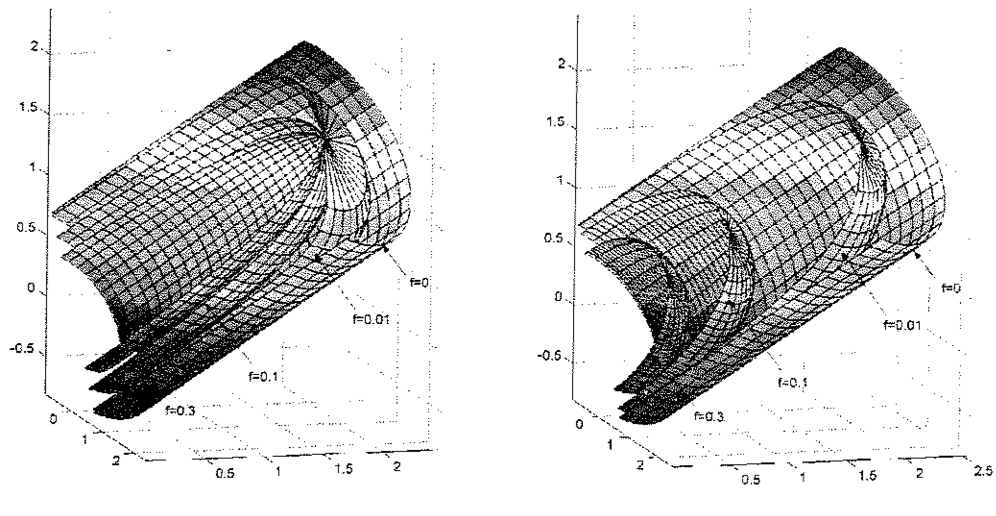


(a) Cohesive micro-crack model (b) The Gurson's model

Fig. 7. Comparison between cohesive crack damage model and the Gurson's model (I): Yield surfaces in 3D stress space

$$\frac{\bar{\mu}}{\mu}=\frac{\dfrac{\bar{E}}{2(1+\bar{\nu})}}{\dfrac{E}{2(1+\nu)}}=\frac{\dfrac{1}{2\mu}}{\dfrac{1}{2\bar{\mu}}}=\frac{\dfrac{1}{2\mu}}{\dfrac{1}{2\mu}+\dfrac{8(1-\nu)}{3\mu}f\dfrac{\left[2-(\dfrac{\Sigma^{\infty}}{\sigma^0})^2\right]}{\left[1-(\dfrac{\Sigma^{\infty}}{\sigma^0})^2\right]^{3/2}}}$$

$$=\frac{1}{1+\dfrac{16(1-\nu)}{3}f\dfrac{2-(\dfrac{\Sigma^{\infty}}{\sigma^0})^2}{\left[1-(\dfrac{\Sigma^{\infty}}{\sigma^0})^2\right]^{3/2}}} \tag{95}$$

Based on Hencky's maximum distortional energy theory [20], the threshold of yielding for a material entering plastic state is measured by its ability to store certain amount of elastic distortional energy. This measure may be reflected in certain equivalency by the true yielded stress , $\sigma_Y$: the material's yield stress in the virgin state, i.e.

$$U_{distortion}=\frac{1}{12\mu}\left[(\Sigma_1-\Sigma_2)^2+(\Sigma_2-\Sigma_3)^2+(\Sigma_3-\Sigma_1)^2\right]=\frac{1}{6\mu}\sigma_Y^2 \tag{96}$$

Define macro-equivalent stress

$$\Sigma_{eq}=\sqrt{\frac{1}{2}\left[\left(\Sigma_{11}^{\infty}-\Sigma_{22}^{\infty}\right)^2+\left(\Sigma_{22}^{\infty}-\Sigma_{33}^{\infty}\right)^2+\left(\Sigma_{33}^{\infty}-\Sigma_{11}^{\infty}\right)^2+6\left(\Sigma_{12}^{\infty 2}+\Sigma_{23}^{\infty 2}+\Sigma_{13}^{\infty 2}\right)\right]}$$

(97)

After damage,

$$U_{distortion} = \frac{\Sigma_{eq}^2}{6\bar{\mu}} \tag{98}$$

The maximum distortional energy criterion becomes

$$\frac{\Sigma_{eq}^2}{\sigma_Y^2} = \frac{\bar{\mu}}{\mu} \tag{99}$$

To this end, a new continuum damage model, in specific a damaged yield surface, is obtained

$$\frac{\Sigma_{eq}^2}{\sigma_Y^2} = \frac{1}{1 + \dfrac{16(1-\nu)f}{3} \dfrac{2 - (\frac{\Sigma^{\infty}}{\sigma^0})^2}{\left[1 - (\frac{\Sigma^{\infty}}{\sigma^0})^2\right]^{3/2}}} \tag{100}$$

Note that the cohesive stress $\sigma^0$ is linked to yield stress $\sigma_Y$ by Eq. (45). For uniform triaxial loading, $\Sigma^{\infty} = \Sigma_m$, the micro-crack damage model becomes

$$\frac{\Sigma_{eq}^2}{\sigma_Y^2} = \frac{1}{1 + \dfrac{16(1-\nu)f}{3} \dfrac{\left[2 - (\frac{\Sigma_m}{\sigma^0})^2\right]}{\left[1 - (\frac{\Sigma_m}{\sigma^0})^2\right]^{3/2}}} \tag{101}$$

and

$$\frac{\Sigma_m}{\sigma^0} = \frac{4}{1 + \left[\left(\dfrac{4}{1-2\nu}\dfrac{\sigma_Y}{\Sigma_m}\right)^2 - 3\right]^{1/2}} \tag{102}$$

Let $\Psi$ be the damaged yield function acting as a potential for the plastic flow. Combining Eqs. (101) and (102), one may derive the following presure-sensitive plastic potential,

$$\Psi(\Sigma_{eq}, \Sigma_m, \sigma_Y) = \frac{\Sigma_{eq}^2}{\sigma_Y^2}\left\{1 + \frac{32(1-\nu)f}{3}\left(1 + \left[\left(\frac{12}{(1-2\nu)}\frac{\sigma_Y}{(\mathbf{\Sigma}:\mathbf{1})}\right)^2 - 3\right]^{1/2}\right)\right.$$

$$\cdot\frac{\Big[\Big(1+\Big[\Big(\frac{12\sigma_Y}{(1-2\nu)(\mathbf{\Sigma}:\mathbf{1})}\Big)^2-3\Big]^{1/2}\Big)^2-8\Big]}{\Big[\Big(1+\Big[\frac{12\sigma_Y}{(1-2\nu)(\mathbf{\Sigma}:\mathbf{1})}\Big]^2-3\Big)^2-16\Big]^{3/2}}\Bigg\}=0 \quad (103)$$

where $\mathbf{\Sigma} = \Sigma_{ij}\mathbf{e}_i \otimes \mathbf{e}_j$ is the macro-stress tensor, and $\mathbf{1} = \delta_{ij}\mathbf{e}_i \otimes \mathbf{e}_j$ is the second order unit tensor.

Consider

$$\Sigma_{eq}^2 = \frac{3}{2}\mathbf{\Sigma}^{dev} : \mathbf{\Sigma}^{dev} \quad (104)$$

$$\mathbf{\Sigma}^{dev} = \mathbf{\Sigma} - \frac{1}{3}trace\big(\mathbf{\Sigma}\big)\mathbf{1} \quad (105)$$

The macro plastic flow direction may be given by the associative rule

$$\mathbf{D}^p = \dot{\lambda}\mathbf{n} \quad (106)$$

where $\mathbf{D}^p = \frac{1}{2}\Big(\dot{u}^p_{i,j} + \dot{u}^p_{j,i}\Big)\mathbf{e}_i \otimes \mathbf{e}_j$. and

$$\mathbf{n} = \frac{\partial\Psi}{\partial\mathbf{\Sigma}} = \frac{3}{\sigma_Y^2}\Big(1 + \frac{16(1-\nu)f}{3}\frac{(2-A^2)}{(1-A^2)^{3/2}}\Big)\mathbf{\Sigma}^{dev}$$
$$+\frac{4\Sigma_{eq}^2(1-\nu)f}{3\sigma_Y^2}\frac{(4-A)A^2}{(1-A^2)^{5/2}}\frac{\Big(\frac{12\sigma_Y}{(1-2\nu)(\mathbf{\Sigma}:\mathbf{1})}\Big)^2}{\Big(\Big[\frac{12\sigma_Y}{(1-2\nu)(\mathbf{\Sigma}:\mathbf{1})}\Big]^2-3\Big)^{1/2}}$$
$$\cdot\frac{\mathbf{1}}{(\mathbf{\Sigma}:\mathbf{1})} \quad (107)$$

where

$$A = \frac{4}{1+\Big(\Big[\frac{12\sigma_Y}{(1-2\nu)(\mathbf{\Sigma}:\mathbf{1})}\Big]^2-3\Big)^{1/2}} \quad (108)$$

The scalar plastic flow rate can be determined by consistency condition as usual,

$$\dot{\lambda} = \frac{\langle \mathbf{r}:\mathbf{C}:\mathbf{D}\rangle}{-\Psi_{\mathbf{q}}\cdot\mathbf{h}+\mathbf{n}\cdot\mathbf{C}\cdot\mathbf{n}} \quad (109)$$

where $\mathbf{C}$ is the elastic tensor, and $< \cdot >$ is the Macauley bracket, and $\mathbf{q}$ are internal variables that are specified as

$$\dot{\mathbf{q}} = \dot{\lambda}\mathbf{h}(\mathbf{\Sigma}, \mathbf{q}) \tag{110}$$

The damage evolution law for micro-cracks in a cohesive elastic environment may be significant from that of voids in a perfectly viscoplastic environment. By assuming that the total rate change of the crack volume is proportional to *the volume rate change in a RVE*, i.e.

$$\dot{V}_c = \alpha \dot{V} \tag{111}$$

Then

$$\dot{f}_{growth} = \frac{d}{dt}\Big(\frac{V_c}{V}\Big) = (\alpha - f)\frac{\dot{V}}{V} = (\alpha - f)trace(\mathbf{D}) \tag{112}$$

If the material is incompressible at macro-level ($\alpha = 1$), and plastic rate of deformation is dominant, the conventional damage evolution law is recovered

$$\dot{f} = (1 - f)trace(\mathbf{D}^p) \tag{113}$$

On the other hand, an argument can be made that since the volume fraction of cohesive cracks is obtained by integrating elastic crack opening displacement (COD), i.e., $f = \dfrac{a^3}{V}$ (for single crack), if one assumes that $\dot{V}_e = \dot{V}_c$

$$\begin{aligned}\dot{f} &= (1 - \alpha^{-1} f)trace(\mathbf{D}^e) = (1 - \alpha^{-1} f)trace(\mathbf{D} - \mathbf{D}^p) \\ &= (1 - \alpha^{-1} f)trace\left(\Big(\mathbf{1} - \frac{(\mathbf{1} : \mathbf{n}) \otimes (\mathbf{n} : \mathbf{C})}{-\Psi_{\mathbf{q}} \cdot \mathbf{h} + \mathbf{n} : \mathbf{C} : \mathbf{n}}\Big) : \mathbf{D}\right)\end{aligned} \tag{114}$$

## 6 Discussions

A distinct nature of this new damage model is that yield loci for different micro-crack volume fraction all arrive at the same point in stress space when $\Sigma_{eq}/\sigma_Y = 0$, i.e. on $\Sigma_m/\sigma_Y$ axis (see Figure 7 and 8 ), which is significantly different from other continuum damage models, for instance, the Gurson's model.

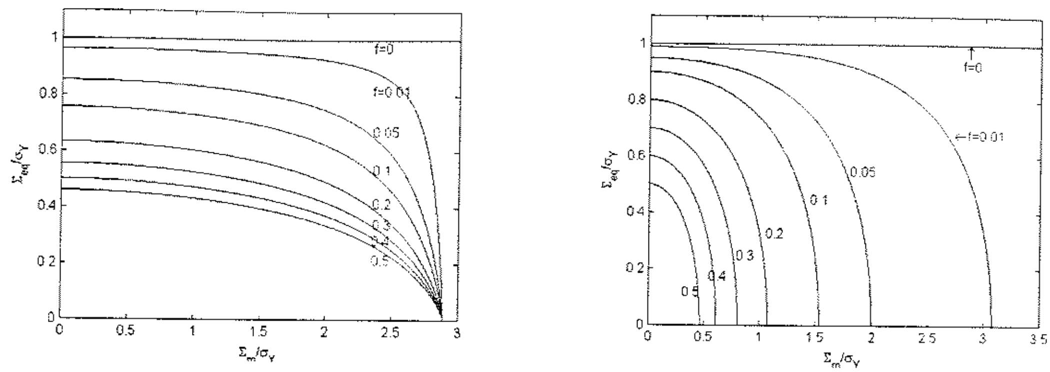


(a) Cohesive crack damage model

(b) The Gurson's model

Fig. 8. Comparison between the cohesive crack damage model and the Gurson's model (II) ($\nu = 0.30$).

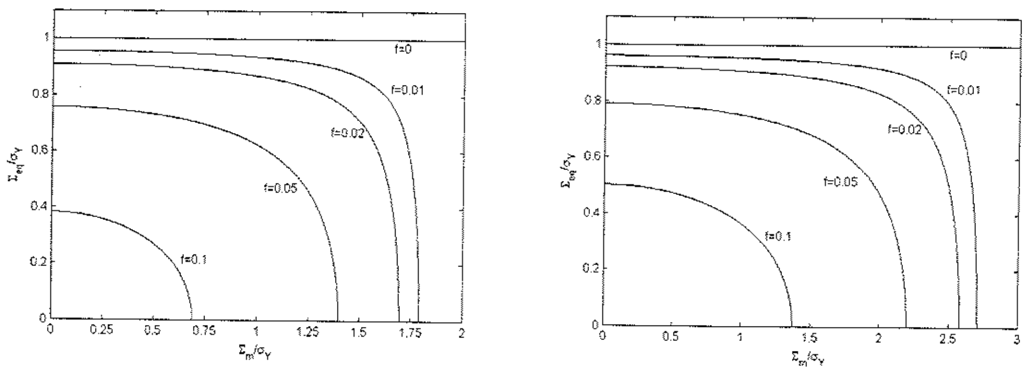


(a) $\nu = 0.2$

(b) $\nu = 0.3$

Fig. 9. Damaged yield loci for dilute cohesive crack distributions.

A plausible explanation of this phenomenon is as follows: if $\Sigma^{\infty} = \Sigma_m \Rightarrow \sigma_0$, the macro-stress reaches the value of cohesion. At that point, the size of the process zone will be infinite, $b \to \infty$, then the material totally losses its physical strength. As shown in Eq. (101), as $\Sigma_m \to \sigma_0$,

$$\frac{\Sigma_{eq}}{\sigma_Y} \to 0 \qquad \frac{\Sigma_m}{\sigma_Y} \to \frac{4}{\sqrt{12}(1-2\nu)} \tag{115}$$

The continuum damage model derived in this paper is under the assumption that the distribution of cohesive micro-crack is dilute, so that the interaction among cracks can be neglected. The assumption will be longer held if the crack volume fraction exceeds certain limit. Under those situations, interaction among cohesive cracks becomes important, and it has to be taken into consideration because it directly leads to crack coalescence.

Based on this argument, when $\Sigma^{\infty} \to \sigma^0$ and $b \to \infty$, the cohesive micro-

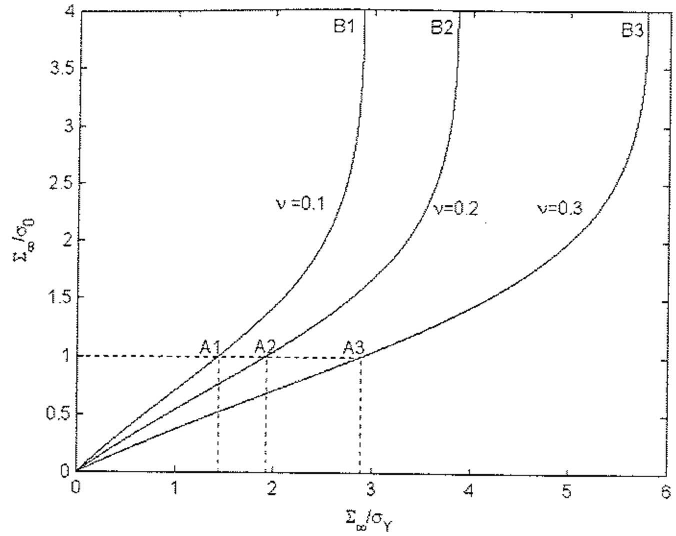


Fig. 10. Relationship between physical cohesion and true yield stress

crack distribution can no longer be viewed as a dilute distribution, discretion on applicability of the damage model in this range is advised.

On the other hand, if cohesive crack distribution is dilute, from Eq. (101), one may adopt the following approximation

$$\Psi(\Sigma_{eq}, \Sigma_m, \sigma_Y) = \frac{\Sigma_{eq}^2}{\sigma_Y^2} + \frac{16(1-\nu)f}{3} \frac{\left[2 - (\frac{\Sigma_m}{\sigma^0})^2\right]}{\left[1 - (\frac{\Sigma_m}{\sigma^0})^2\right]^{3/2}} - 1 + \mathcal{O}(f^2) = 0 \ , \tag{116}$$

where the parameter $\Sigma_m/\sigma^0$ is determined by Eq. 102. Interestingly, this approximated solution is probably more closer to reality than the closed form solution presented in (101), since it confines itself under the restriction of dilute crack distribution, whereas Eq. 101 is only justified in dilute crack distribution while attemping to cover a large range of crack volume fraction.

Under this approximation, the damaged yield loci do not converge to one point as they approach to the $\Sigma_m/\sigma_Y$ axis (see Fig. 9).

In fact, the damage due to interaction of cohesive micro-cracks has been attracted some attentions, e.g. Feng and Gross [13]. We speculated that in general by considering interaction induced coalescence among cohesive cracks, the yield loci with different micro-crack volume fractions will not converge to a same point in stress space as $\Sigma_{eq}/\sigma_Y = 0$. The continuum damage model, or evolution with rich micro-crack distribution is currently under investigation.

Finally, one may notice that Eq. (45) gives a relationship between physical cohesion, $\sigma^0$, and the true (micro) yield stress, $\sigma_Y$,

$$\frac{\Sigma^\infty}{\sigma_0} = \frac{4}{1 + \sqrt{\left(\frac{4}{1-2\nu}\frac{\sigma_Y}{\Sigma^\infty}\right)^2 - 3}} \tag{117}$$

It gave an impression that the relationship between the two parameters depends on the macro-hydrostatic stress state, $\Sigma^\infty$.

To provide the insight of this relationship, Eq. (117) is plotted with different Poisson's ratio in Fig. 10. One may find that when $\Sigma^\infty/\sigma_Y < 2$, the physical cohesion is almost proportional to yield stress,

$$\sigma^0 \approx \frac{4}{\sqrt{12}(1-2\nu)}\sigma_Y \tag{118}$$

Therefore for all practical concerns, $\sigma_Y$ being constant will imply the constancy of physical cohesion, or vice versa.

## Acknowledgements

The authors would like to acknowledge Mr. Wei-Kang Lee's early participation in this research project. The work is supported by an Junior Faculty Research Fund (BURNL-07427-11503-EGSLI) provided by the senate committee on research in University of California at Berkeley.

## References

[1] G. I. Barenblatt. The formation of equilibrium cracks during brittle fracture. *J. Appl. Math. & Mechanics, [English translation PMM, Vol. 23, 434]*, 23:622, 1959.

[2] G. I. Barenblatt. The mathematical theory of equilibrium cracks in brittle fracture. In *Advances in Applied Mechanics*, volume 7, pages 55–129. Academic Press, 1962.

[3] W. Becker and D. Gross. About the mode ii dugdale crack solution. *International Journal of Fracture*, 34:65–70, 1987.

[4] W. Becker and D. Gross. A one-dimensional micromechanical model of elastic-microplastic damage evolution. *Acta Mechanica*, 70:221–233, 1987.

[5] W. Becker and D. Gross. About the dugdale crack under mixed mode loading. *International Journal of Fracture*, 37:163–170, 1988.

[6] W. Becker and D. Gross. About the penny-shaped dugdale crack under shear and triaxial loading. In *Proceedings of The Seventh International Conference on Fracture (ICF7)*, pages 2289–2299. 1989.

[7] B. A. Bilby, A. H. Cottrell, and K. H. Swinden. The spread of plastic yield from a notch. *Proceedings of Royal Society of London, Series A*, 272:304–314, 1963.

[8] W. R. Chen and L. M. Keer. Fatigue crack growth in mixed mode loading. *ASME Journal of Engineering Materials and Technology*, 113:222–227, 1991.

[9] W. R. Chen and L. M. Keer. Mixed-mode fatigue crack propagation of penny-shaped cracks. *ASME Journal of Engineering Materials and Technology*, 115:365–372, 1993.

[10] D. S. Dugdale. Yielding of steel sheets containing slits. *Journal of Mechanics and Physics of Solids*, 8:100–104, 1960.

[11] J. D. Eshelby. The determination of the elastic field of an ellipsoidal inclusion, and related problems. *Proc. R. Soc. London, Ser. A.*, 241:376–396, 1957.

[12] J. D. Eshelby. The elastic field outside an ellipsoidal inclusion. *Proc. R. Soc. London, Ser. A.*, 252:561–569, 1959.

[13] X.-Q. Feng and D. Gross. On the coalescence of collinear cracks in quasi-brittle materials. *Engineering Fracture Mechanics*, 65:511–524, 2000.

[14] H. Gao and P. Klein. Numerical simulation of crack growth in an isotropic solid with randomized internal cohesive bonds. *Journal of Mechanics and Physics of Solids*, 46:187–218, 1999.

[15] A. E. Green and W. Zerna. *Theoretical Elasticity*. Oxford University Press, Oxford, U.K., 1968.

[16] A. L. Gurson. *Plastic Flow and Fracture Behavior of Ductile Materials Incorporating Void Nucleation, Growth and Interaction*. PhD thesis, Brown University, 1975.

[17] A. L. Gurson. Continuum theory of ductile rupture by void nucleation and growth: Part i yield criteria and flow rules for porous ductile materials. *Journal of Engineering Materials and Technology*, 99:2–15, 1977.

[18] Z. Hashin and S. Shtrikman. On some variational principles in anisotropic and nonhomogeneous elasticity. *Jopurnal of the Mechanics and Physics of Solids*, 10:335–342, 1962.

[19] Z. Hashin and S. Shtrikman. A variational approach to the theory of the elastic behaviour of polycrystals. *Jopurnal of the Mechanics and Physics of Solids*, 10:343–352, 1962.

[20] Von H. Hencky. Zur theorie plastischer deformationen und der hierdurch im material hervorgerufen nachspannungen. *Zeits. ang. Math. Mech.*, 4:323–334, 1924.

[21] R. Hill. Elastic properties of reinforced solids: Some theoretical principles. *Journal of the Mechanics and Physics of Solids*, 11:357–372, 1963.

[22] M. Kachanov. Effective elastic properties of cracked solids: Critical review of some basic concepts. *Applied Mechanics Review*, 45:304–335, 1992.

[23] M. Kachanov. Elastic solids with many cracks and related problems. In J. W. Hutchinson and T. Y. Wu, editors, *Advances in Applied Mechanics*, pages 259–445. Academic Press, New York, 1994.

[24] M. K. Kassir and G. C. Sih. *Mechanics of Fracture: Three-dimensional Crack Problems*, volume 2. Noordhoff International Publishing, Leyden, 1975.

[25] L. M. Keer and T. Mura. Stationary crack and continuous distributions of dislocations. In *Proceedings of The First International Conference on Fracture*, volume 1, pages 99–115. The Japanese Society for Strength and Fracture of Materials, 1965.

[26] D. Krajcinovic. *Damage Mechanics*. Elsevier, Amsterdam · New York, 1996.

[27] T. J. Lu and C. L. Chow. A modified dudgale model for crack tip plasticity and its related problems. *Engineering Fracture Mechanics*, 37:551–568, 1990.

[28] F. A. McClintock. A criterion for ductile fracture by the growth of holes. *ASME Journal of Applied Mechanics*, 35:363–371, 1968.

[29] T. Mura. *Micromechanics of Defects in Solids*. Martinus Nijhoff Publishers, Dordrecht, 1987.

[30] S. Nemat-Nasser and M. Hori. Elastic solids with microdefects. In G. J. Weng, M. Taya, and H. Abe, editors, *Micromechanics and Inhomogeneity*, pages 297–320. Springer-Verlag, New York, 1990.

[31] S. Nemat-Nasser and M. Hori. *Micromechanics: overall properties of heterogeneous materials*. Elsevier, Amsterdam-Lausanne-New York-Oxford-Singapore-Tokyo, 1999.

[32] M. Ortiz and A. Pandolfi. Finite-deformation irreversible cohesive elements for three-dimensional crack-propagation analysis. *International Journal for Numerical Methods in Engineering*, 44:1267–1282, 1999.

[33] J. R. Rice. Dislocation nucleation from a crack tip: An analysis based on the peierles concept. *Journal of Mechanics and Physics of Solids*, 40:239–271, 1992.

[34] J. R. Rice and R. Thomson. Ductile versu brittle behavior of crystals. *Philosophical Magazine*, 29:73–97, 1974.

[35] V. Tvergaard. Material failure by void growth to coalescence. In J. W. Hutchinson and T. Y. Wu, editors, *Advances in Applied Mechanics*, volume 27, pages 83–151. Academic Press, New York, 1990.

[36] J. Weertman. *Dislocation Based Fracture Mechanics*. World Scientific, Singapore · New Jersey · Hong Kong, 1996.

[37] P. Xu and A. Needleman. Numerical simulations of fast crack growth in brittle solids. *Journal of the Mechanics and Physics of Solids*, 42:1397–1434, 1994.